Inorg. Chem. **2005**, *44*, 6092–6099

Complex Series $[Ru(tpy)(dpk)(X)]^{n+}$ (tpy = 2,2′:6′,2″-Terpyridine; dpk = 2,2′-Dipyridyl Ketone; X = Cl^-, CH_3CN, NO_2^-, NO^+, $NO^\bullet$, NO^-): Substitution and Electron Transfer, Structure, and Spectroscopy

Sounak Sarkar,[†] Biprajit Sarkar,[‡] Nripen Chanda,[†] Sanjib Kar,[†] Shaikh M. Mobin,[†] Jan Fiedler,[§] Wolfgang Kaim,*[,‡] and Goutam Kumar Lahiri*[,†]

Department of Chemistry, Indian Institute of Technology—Bombay, Powai, Mumbai-400076, India, Institut für Anorganische Chemie, Universität Stuttgart, Pfaffenwaldring 55, D-70550 Stuttgart, Germany, and J.Heyrovsky Institute of Physical Chemistry, Academy of Sciences of the Czech Republic, Dolejškova 3, CZ-18223 Prague, Czech Republic

Received April 7, 2005

The complex framework $[Ru(tpy)(dpk)]^{2+}$ has been used to study the generation and reactivity of the nitrosyl complex $[Ru(tpy)(dpk)(NO)]^{3+}$ ([**4**]$^{3+}$). Stepwise conversion of the chloro complex $[Ru(tpy)(dpk)(Cl)]^+$ ([**1**]$^+$) via $[Ru(tpy)(dpk)(CH_3CN)]^{2+}$ ([**2**]$^{2+}$) and the nitro compound $[Ru(tpy)(dpk)(NO_2)]^+$ ([**3**]$^+$) yielded [**4**]$^{3+}$; all four complexes were structurally characterized as perchlorates. Electrochemical oxidation and reduction was investigated as a function of the monodentate ligand as was the IR and UV–vis spectroscopic response (absorption/emission). The kinetics of the conversion [**4**]$^{3+}$/[**3**]$^+$ in aqueous environment were also studied. Two-step reduction of [**4**]$^{3+}$ was monitored via EPR, UV–vis, and IR (ν(NO), ν(CO)) spectroelectrochemistry to confirm the $\{RuNO\}^7$ configuration of [**4**]$^{2+}$ and to exhibit a relatively intense band at 505 nm for [**4**]$^+$, attributed to a ligand-to-ligand transition originating from bound NO^-.

Introduction

There is intense renewed interest in nitrosyl chemistry, primarily due to its relevance for biological[1] and environmental[2] processes. The important biological activities of nitric oxide ($NO^\bullet$) include cardiovascular control,[3] neuronal signaling,[4] and its role in defense mechanisms against microorganisms and tumors.[5] In this context, a variety of ruthenium–nitrosyl complexes have also been explored in recent years as possible therapeutic agents.[6] By virtue of its unique noninnocent ligand characteristics, nitric oxide can readily shuttle between the three possible redox states NO^+, $NO^\bullet$, and NO^-, depending on the electronic nature of the coligands L_n associated with the metal–nitrosyl fragment in $[L_nM(NO)]$. For example, the NO^+ state exists in metmyoglobin as $Fe^{II}-NO^+$[7] and the NO^- state is being discussed for reduced vitamin B_{12} in the form of a $Co^{III}-NO^-$ entity.[8] Moreover, the electrophilic $M-NO^+$ [ν(NO) > 1900 cm^{-1}] moiety is drawing special attention since coordinated NO^+ is known to undergo a variety of molecular transformations on nucleophilic attack.[9] The degree of electrophilicity of coordinated $M-NO^+$ can be systematically tuned through the modulation of ancillary functions in the complex matrixes. Thus, substantial variation of the ν(NO) frequency

* Authors to whom correspondence should be addressed. E-mail: lahiri@chem.iitb.ac.in (G.K.L.); kaim@iac.uni-stuttgart.de (W.K.).
† Indian Institute of Technology—Bombay.
‡ Universität Stuttgart.
§ Academy of Sciences of the Czech Republic.

(1) (a) Howard, J. B.; Rees, D. C. *Chem. Rev.* **1996**, *96*, 2965. (b) Burgees, B. K.; Lowe, D. J. *Chem. Rev.* **1996**, *96*, 2983. (c) Eady, R. R. *Chem. Rev.* **1996**, *96*, 3013. (d) Stamler, J. S.; Singel, D. J.; Loscalzo, J. *Science* **1992**, *258*, 1898. (e) Culotta, E.; Koshland, D. E., Jr. *Science* **1992**, *258*, 1862. (f) Pfeiffer, S.; Mayer, B.; Hemmens, B. *Angew. Chem., Int. Ed.* **1999**, *38*, 1714. (g) Richter-Addo, G. B.; Legzdins, P.; Burstyn, J. C*hem. Rev.* **2002**, *102*, No.4. (h) Moncada, S.; Palmer, R. M. J.; Higgs, E. A. *Pharmacol. Rev.* **1991**, *43*, 109. (i) Ritcher-Addo, G. B.; Legzdins, P. In *Metal Nitrosyls*; Oxford University Press: New York, 1992. (j) Scheidt, W. R.; Ellison, M. K. *Acc. Chem. Res.* **1999**, *32*, 350. (k) Cooper, C. E. *Biochim. Biophys. Acta* **1999**, *1411*, 290. (l) Wieraszko, A.; Clarke, M. J.; Lang, D. R.; Lopes, L. G. F.; Franco, D. W. *Life Sci.* **2001**, *68*, 1535. (m) Patra, A. K.; Mascharak, P. K. *Inorg. Chem.* **2003**, *42*, 7363. (n) Ghosh, K.; Eroy-Reveles, A. A.; Avila, B.; Holman, T. R.; Olmstead, M. M.; Mascharak, P. K. *Inorg. Chem.* **2004**, *43*, 2988. (o) Patra, A. K.; Rose, M. J.; Murphy, K. A.; Olmstead, M. M.; Mascharak, P. K. *Inorg. Chem.* **2004**, *43*, 4487.

(2) (a) Pandey, K. K. *Coord. Chem. Rev.* **1983**, *51*, 69. (b) Zang, V.; van Eldik, R. *Inorg.Chem.* **1990**, *29*, 4462. (c) Pham, E. K.; Chang, S. G. *Nature* **1994**, *369*, 139.
(3) Calver, A.; Collier, J.; Vallance, P. *Exp. Physiol.* **1993**, *78*, 303.
(4) Ignarro, L. J. *Hypertension* **1990**, *16*, 477.
(5) Snyder, S. H.; Bredt, D. S. *Sci. Am.* **1992**, *266*, 68.

10.1021/ic050533e CCC: $30.25
Published on Web 07/21/2005

in $[(L)(tpy)Ru^{II}(NO)]^{3+}$ (tpy = 2,2′:6′,2″-terpyridine) has been achieved by changing the π-acid and σ-donor properties of L.[10−15] This has initiated the present program of introduction of a symmetrical pyridyl-based heterocycle, 2,2′-dipyridyl ketone (dpk), as ancillary ligand (L) to the $\{Ru(tpy)(NO)\}^{3+}$ core to investigate the effect of dpk on the stability of coordinated NO in different redox states.

Herein we report the stepwise synthesis, X-ray structures, and spectroelectrochemical properties of the complexes $[Ru(tpy)(dpk)(Cl)](ClO_4) = [\mathbf{1}](ClO_4) \rightarrow [Ru(tpy)(dpk)(CH_3CN)](ClO_4)_2 = [\mathbf{2}](ClO_4)_2 \rightarrow [Ru(tpy)(dpk)(NO_2)](ClO_4) = [\mathbf{3}](ClO_4) \rightarrow [Ru(tpy)(dpk)(NO)](ClO_4)_3 = [\mathbf{4}](ClO_4)_3$. The spectroscopic and electrochemical features of the nitrosyl derivative $[\mathbf{4}]^{n+}$ in different accessible redox states ($n = 3$, 2, 1) have been examined by spectroelectrochemical (UV−vis−IR) and EPR investigations. The reactivity of $[\mathbf{4}](ClO_4)_3$ in the presence of water as nucleophile and the corresponding kinetic aspects have also been studied.

Results and Discussion

Synthesis and Characterization. The nitrosyl complex $[\mathbf{4}](ClO_4)_3$ was prepared in a sequential manner starting from $[Ru(tpy)(dpk)(Cl)](ClO_4) = [\mathbf{1}](ClO_4)$ via $[Ru(tpy)(dpk)(CH_3CN)](ClO_4)_2 = [\mathbf{2}](ClO_4)_2$ and $[Ru(tpy)(dpk)(NO_2)]ClO_4 = [\mathbf{3}](ClO_4)$ (Scheme 1). Synthesis of the nitrosyl species $[\mathbf{4}](ClO_4)_3$ directly from the precursors $[\mathbf{1}](ClO_4)$ or $[\mathbf{2}](ClO_4)_2$ by using NO gas had failed; therefore, the sequential synthetic route was adopted (Scheme 1).

Scheme 1 [a]

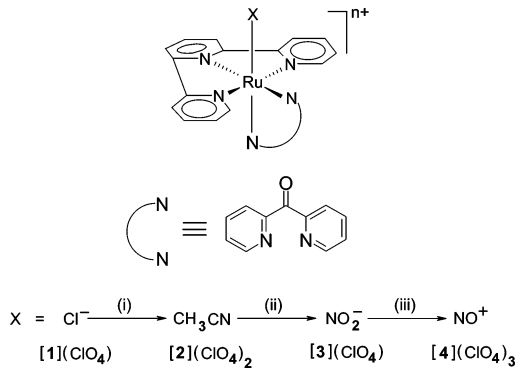

[a] Key: (i) excess $AgNO_3$ in CH_3CN/H_2O (1:5)/reflux; (ii) excess $NaNO_2$ in water/reflux; (iii) concentrated $HNO_3/HClO_4$, stir at 273 K/water.

Though dpk is known to bind with metal ions either in a symmetrical bidentate mode via the pyridyl nitrogen donor centers[16] or by using one of the pyridyl nitrogen atoms and the carbonyl oxygen,[17] only the N,N′ binding mode of dpk was observed in the present set of complexes. Although the C═O group of Ru-coordinated dpk was reported to undergo transformation to $C(OH)_2$ in the presence of Ag^+/H_2O,[18] no such transformation was observed during the reaction of $[\mathbf{1}](ClO_4)$ with Ag^+ in CH_3CN-H_2O (1:5); instead, solvolysis of Ru−Cl to Ru−CH_3CN took place (see later).

The formation of the complexes was authenticated by molar conductance, microanalytical, IR, ^1H NMR, and electrospray mass spectral data (see the Experimental Section and Table 3). The crystal structures of $[\mathbf{1}](ClO_4)$ (crystallized as a monohydrate), $[\mathbf{2}](ClO_4)_2$, $[\mathbf{3}](ClO_4)$, and $[\mathbf{4}](ClO_4)_3$ (crystallized as a bis(acetonitrile) solvate) are shown in Figures 1−4. Selected crystallographic and structural parameters are listed in Tables 1 and 2, respectively. In the complexes, the tpy ligand is coordinated to the ruthenium ion in the expected meridional fashion with the dpk ligand N,N′ chelating in a cis position.[19] The geometrical constraints due to the meridional binding of tridentate tpy are reflected

(6) (a) Karidi, K.; Garoufis, A.; Tsipis, A.; Hadjiliadis, N.; Dulk, H. D.; Reedijk, J. *Dalton Trans*. **2005**, 1176. (b) Fricker, S. P.; Slade, E.; Powell, N. A.; Vaughn, O. J.; Henderson, G. R.; Murrer, S. A.; Megson, I. C.; Bisland, S. K.; Flitney, F. W. *Br. J. Pharmacol*. **1997**, *122*, 1441. (c) Carter, T. D.; Bettache, N.; Ogden, D. *Br. J. Pharmacol.* **1997**, *122*, 971. (d) Ackroyd, R.; Kelty, C.; Brown, N.; Reed, M. *Photochem. Photobiol.* **2001**, *74*, 656. (e) Bettache, N.; Carter, T.; Corrie, J. E. T.; Ogden, D.; Trentham, D. R. In *Methods in Enzymology*; Packer, L., Ed.; Academic Press: San Diego, CA 1996; Vol. 268, p 266. (f) Davies, N.; Wilson, M. T.; Slade, E.; Fricker, S. P.; Murrer, B. A.; Powell, N. A.; Henderson, G. R. *J. Chem. Soc., Chem. Commun*. **1997**, 47. (g) Chen, Y.; Shepherd, R. E. *J. Inorg. Biochem*. **1997**, *68*, 183. (h) Slocik, J. M.; Ward, M. S.; Shepherd, R. E. *Inorg. Chim. Acta* **2001**, *317*, 290. (i) Lopes, L. G. F.; Wieraszko, A.; El-Sherif, Y.; Clarke, M. J. *Inorg. Chim. Acta* **2001**, *312*, 15. (j) Slocik, J. M.; Shepherd, R. E. *Inorg. Chim. Acta* **2000**, *311*, 80. (k) Bezerra, C. W. B.; Silva, S. C.; Gambardella, M. T. P.; Santos, R. H. A.; Plicas, L. M. A.; Tfouni, E.; Franco, D. W. *Inorg. Chem*. **1999**, *38*, 5660. (l) Lang, D. R.; Davis, J. A.; Lopes, L. G. F.; Ferro, A. A.; Vasconcellos, L. C. G.; Franco, D. W.; Tfouni, E.; Wieraszko, A.; Clarke, M. J. *Inorg. Chem.* **2000**, *39*, 2294. (m) Hui, J. W.-S.; Wong, W.-T. *Coord. Chem. Rev*. **1998**, *172*, 389. (n) Lee, S.-M.; Wong, W.-T. *Coord. Chem. Rev*. **1997**, *164*, 415. (o) Ford, P. C.; Bourassa, J.; Miranda, K.; Lee, B.; Lorkovic, I.; Boggs, S.; Kudo, S.; Laverman, L. *Coord. Chem. Rev.* **1998**, *171*, 185. (p) Tfouni, E.; Krieger, M.; McGarvey, B. R.; Franco, D. W. *Coord. Chem. Rev.* **2003**, *236*, 57.
(7) Laverman, L. E.; Wanat, A.; Oszajca, J.; Stochel, G.; Ford, P. C.; van Eldik, R. *J. Am. Chem. Soc*. **2001**, *123*, 285.
(8) Wolak, M.; Stochel, G.; Zahl, A.; Schneppensieper, T.; van Eldik, R. *J. Am. Chem. Soc*. **2001**, *123*, 9780.
(9) (a) McCleverty, J. A. *Chem. Rev*. **1979**, *79*, 53. (b) Das, A.; Jones, C. J.; McCleverty, J. A. *Polyhedron* **1993**, *12*, 327. (c) Thiemens, M. H.; Trogler, W. C. *Science* **1991**, *251*, 932. (d) Feelisch, M., Stamler, J. S., Eds. *Methods in Nitric Oxide Research*; Wiley: Chichester, U.K., 1996. (e) Enemark, J. H.; Felthan, R. D. *Coord. Chem. Rev*. **1974**, *13*, 339. (f) Chakravarty, A. R.; Chakravorty, A. *J. Chem. Soc., Dalton Trans.* **1983**, 961. (g) Byabartta, P.; Jasimuddin, Sk.; Ghosh, B. K.; Sinha, C.; Slawin, A. M. Z.; Woollins, J. D. *New J. Chem.* **2002**, *26*, 1415. (h) Olabe, J. A. *Adv. Inorg. Chem.* **2004**, *55*, 61.
(10) Mondal, B.; Paul, H.; Puranik, V. G.; Lahiri, G. K. *J. Chem. Soc., Dalton Trans*. **2001**, 481.
(11) Chanda, N.; Paul, D.; Kar, S.; Mobin, S. M.; Datta, A.; Puranik, V. G.; Rao, K. K.; Lahiri, G. K. *Inorg. Chem.* **2005**, *44*, 3499.
(12) Pipes, D. W.; Meyer, T. J. *Inorg. Chem*. **1984**, *23*, 2466.
(13) Chanda, N.; Mobin, S. M.; Puranik, V. G.; Datta, A.; Niemeyer, M.; Lahiri, G. K. *Inorg. Chem.* **2004**, *43*, 1056.
(14) Dovletoglou, A.; Adeyemi, S. A.; Meyer, T. J. *Inorg. Chem*. **1996**, *35*, 4120.
(15) Hadadzadeh, H.; DeRosa, M. C.; Yap, G. P. A.; Rezvani, A. R.; Crutchley, R. J. *Inorg. Chem*. **2002**, *41*, 6521.
(16) (a) Madureira, J.; Santos, T. M.; Goodfellow, B. J.; Lucena, M.; Pedrosa de Jesus, J.; Santana-Marques, M. G.; Drew, M. G. B.; Felix, V. *J. Chem. Soc., Dalton Trans.* **2000**, 4422. (b) Bakir, M.; McKenzie, J. A. M. *J. Chem. Soc., Dalton Trans.* **1997**, 3571. (c) Paik Suh, M.; Kwak, C.-H.; Suh, J. *Inorg. Chem*. **1989**, *28*, 50. (d) Dessy, R. E.; Charkoudian, J. C.; Rheingold, A. L. *J. Am. Chem. Soc*. **1972**, *94*, 738. (e) Miller, J. M.; Balasanmugam, K.; Nye, J.; Deacon, G. B.; Thomas, N. C. *Inorg. Chem*. **1987**, *26*, 560.
(17) (a) Bellachioma, G.; Cardaci, G.; Gramlich, V.; Macchioni, A.; Valentini, M.; Zuccaccia, C. *Organometallics* **1998**, *17*, 5025 (b) Godard, C.; Duckett, S. B.; Parsons, S.; Perutz, R. N. *Chem. Commum*. **2003**, 2332.
(18) (a) Crowder, K. N.; Garcia, S. J.; Burr, R. L.; North, J. M.; Wilson, M. H.; Conley, B. L.; Fanwick, P. E.; White, P. S.; Sienerth, K. D.; Granger, R. M. *Inorg. Chem*. **2004**, *43*, 72. (b) Basu, A.; Kasar, T. G.; Sapre, N. Y. *Inorg. Chem*. **1988**, *27*, 4539. (c) Bhaduri, S.; Sapre, N. Y.; Jones, P. G. *J. Chem. Soc., Dalton Trans.* **1991**, 2539. (d) Deveson, A. C.; Heath, S. L.; Harding, C. J.; Powell, A. K. *J. Chem. Soc., Dalton Trans.* **1996**, 3173.

Table 1. Crystallographic Data

param	[**1**](ClO$_4$)·H$_2$O	[**2**](ClO$_4$)$_2$	[**3**](ClO$_4$)	[**4**](ClO$_4$)$_3$·2CH$_3$CN
molecular formula	$C_{26}H_{21}Cl_2N_5O_6Ru$	$C_{28}H_{22}Cl_2N_6O_9Ru$	$C_{26}H_{19}ClN_6O_7Ru$	$C_{30}H_{25}Cl_3N_8O_{14}Ru$
fw	671.45	758.49	663.99	929.00
radiatn	Mo Kα	Mo Kα	Mo Kα	Mo Kα
cryst sym	monoclinic	triclinic	monoclinic	monoclinic
space group	*C*2/*c*	$P\bar{1}$	$P2_1/n$	$P2_1/c$
a (Å)	30.698(4)	10.095(14)	8.6950(7)	12.994(8)
b (Å)	7.9640(11)	11.130(11)	19.8760(19)	17.396(3)
c (Å)	22.463(3)	13.991(2)	15.630(3)	16.5140(10)
α (deg)	90.0	80.70(13)	90.0	90
β (deg)	106.066(10)	75.70(11)	105.503(11)	97.00(4)
γ (deg)	90.0	84.44(15)	90.0	90.0
V (Å^3)	5277.2(11)	1500.6(4)	2602.9(5)	3691(2)
Z	8	2	4	4
μ (mm^{-1})	0.849	0.765	0.764	0.720
T (K)	293(2)	293(2)	293(2)	293(2)
D_{calcd} (g cm^{-3})	1.690	1.679	1.694	1.672
2*θ* range (deg)	2.76−49.90	3.04−49.94	3.38−49.86	3.16−49.90
e data (R_{int})	4647 (0.0211)	5243 (0.0372)	4572 (0.0193)	6424 (0.1065)
R1 ($I > 2\sigma(I)$)	0.0346	0.0573	0.0444	0.0671
wR2 (all data)	0.0939	0.1566	0.1278	0.2114
GOF	1.051	1.027	1.057	0.909

Table 2. Selected Bond Distances (Å) and Angles (deg) for the Complexes

bond length/ bond angle	[**1**](ClO$_4$) (X = Cl)	[**2**](ClO$_4$)$_2$ (X = N6)	[**3**]ClO$_4$ (X = N6)	[**4**](ClO$_4$)$_3$ (X = N6)
Ru−X	2.3940(11)	2.044(5)	2.033(4)	1.764(7)
Ru−N1	2.058(3)	2.067(5)	2.103(4)	2.108(6)
Ru−N2	2.085(3)	2.095(5)	2.084(4)	2.114(7)
Ru−N3	2.074(3)	2.096(5)	2.084(4)	2.124(13)
Ru−N4	1.959(3)	1.965(5)	1.961(4)	1.990(10)
Ru−N5	2.082(3)	2.070(5)	2.066(4)	2.154(12)
N6−O2			1.233(6)	1.126(8)
N6−O3			1.247(5)	
N6−C27		1.120(8)		
C27−C28		1.463(9)		
C6−O1	1.212(5)	1.211(8)	1.216(6)	1.178(16)
N1−Ru−X	178.53(9)	178.0(2)	177.97(17)	174.2(5)
N2−Ru−X	91.07(9)	90.2(2)	92.01(16)	90.4(3)
N3−Ru−X	87.97(9)	91.1(2)	87.56(16)	95.6(5)
N4−Ru−X	88.19(9)	89.5(2)	87.90(16)	95.4(3)
N5−Ru−X	87.02(9)	87.8(2)	90.00(17)	90.0(4)
N1−Ru−N2	87.79(12)	88.0(2)	87.50(15)	86.5(3)
N1−Ru−N3	93.16(12)	90.14(19)	90.59(15)	89.8(4)
N1−Ru−N4	92.93(12)	92.4(2)	92.59(15)	87.8(3)
N1−Ru−N5	92.24(12)	91.7(2)	92.03(15)	85.8(4)
N2−Ru−N3	102.13(13)	100.8(2)	100.72(16)	98.6(5)
N2−Ru−N4	178.29(13)	179.6(2)	179.77(16)	174.0(3)
N2−Ru−N5	98.56(13)	100.9(2)	99.59(16)	101.4(4)
N3−Ru−N4	79.38(13)	79.0(2)	79.49(16)	79.6(7)
N3−Ru−N5	158.79(13)	158.2(2)	159.62(16)	159.1(4)
N4−Ru−N5	79.87(13)	79.3(2)	80.20(17)	79.9(6)
C5−C6−C7	121.0 (4)	120.6(6)	121.3(4)	118.0(14)
O2−N6−Ru			121.5(3)	173.1(12)
O3−N6−Ru			120.4(3)	
C27−N6−Ru		175.4(5)		
C28−C27−N6		176.5(8)		

by the intraligand trans angles N3−Ru−N5 of 158.79(13), 158.2(2), 159.62(16), and 159.1(4)° in [**1**](ClO$_4$), [**2**](ClO$_4$)$_2$, [**3**](ClO$_4$), and [**4**](ClO$_4$)$_3$, respectively. The other two interligand trans angles N2−Ru−N4 and N1−Ru-X remain close to 180° for all four complexes. As in other Ru−tpy derivatives,[19,20] the central Ru−N4(tpy) bond lengths of 1.959(3), 1.965(5), 1.961(4), and 1.990(10) Å in [**1**](ClO$_4$), [**2**](ClO$_4$)$_2$, [**3**](ClO$_4$), and [**4**](ClO$_4$)$_3$, respectively, are significantly shorter than the corresponding terminal Ru−N(tpy) distances Ru−N3 [2.074(3), 2.096(5), 2.084(4), and 2.124(13) Å] and Ru−N5 [2.082(3), 2.070(5), 2.066(4), and 2.154(12) Å]. The coordinated dpk ligand is nonplanar, and the two pyridine rings exhibit quite similar dihedral angles of 42.29(0.2), 41.67(0.28), 43.75(0.19), and 46.03(0.42)° in [**1**](ClO$_4$), [**2**](ClO$_4$)$_2$, [**3**](ClO$_4$), and [**4**](ClO$_4$)$_3$, respectively. The Ru−Cl and Ru−N(dpk/tpy) bond distances and the associated angles are in good agreement with reported data on related molecules.[17a,19,20] The coordinated acetonitrile molecule in [**2**](ClO$_4$)$_2$ is in its usual, nearly linear mode with an N6−C27−C28 angle of 176.5(8)°.[21] The NO_2^- ion is bonded via N (as nitro ligand) in agreement with the characteristics of ruthenium(II). The RuN_5Cl and RuN_6 coordination structures in [**1**](ClO$_4$) and in [**2**](ClO$_4$)$_2$, [**3**](ClO$_4$), and [**4**](ClO$_4$)$_3$, respectively, exhibit distorted octahedral geometry as can be seen from the angles subtended at the metal (Table 2). The Ru−N(nitrosyl) bond length of 1.764(7) Å in [**4**](ClO$_4$)$_3$ is comparable with that in other structurally characterized ruthenium−terpyridine−nitrosyl complexes.[11,13,15] The *π*-acceptor character of the NO^+ moiety in [**4**](ClO$_4$)$_3$ is evident from the triple bond length for N(6)−O(2) at 1.126(8) Å as well as from the Ru−N(6)−O(2) angle of 173.1(12)°.

In the crystal of [**1**](ClO$_4$)·H$_2$O, there is weak intermolecular C−H---O interaction between (i) oxygen atoms of perchlorate and C−H groups of the pyridyl rings of dpk and between (ii) the carbonyl oxygen atom of dpk and C−H groups of the pyridyl rings of tpy (Figure S1, Table S1). In [**2**](ClO$_4$)$_2$, C−H---O interactions involving oxygen atoms of the perchlorate and pyridyl ring C−H groups of tpy are observed (Figure S2, Table S2). In [**3**](ClO$_4$), there are C−H---O interactions between oxygen atoms of the per-

(19) Patra, S.; Sarkar, B.; Ghumaan, S.; Patil, M. P.; Mobin, S. M.; Sunoj, R. B.; Kaim, W.; Lahiri, G. K. *Dalton Trans.* **2005**, 1188.

(20) (a) Mondal, B.; Puranik, V. G.; Lahiri, G. K. *Inorg. Chem.* **2002**, *41*, 5831. (b) Chanda, N.; Mondal, B.; Puranik, V. G.; Lahiri, G. K. *Polyhedron* **2002**, *21*, 2033. (c) Catalano, V. J.; Heck, R. A.; Ohman, A.; Hill, M. G. *Polyhedron* **2000**, *19*, 1049. (d) Catalano, V. J.; Heck, R. A.; Immoos, C. E.; Ohman, A.; Hill, M. G. *Inorg. Chem.* **1998**, *37*, 2150.

(21) (a) Rasmussen, S. C.; Ronco, S. E.; Mlsna, D. A.; Billadeau, M. A.; Pennington, W. T.; Kolis, J. W.; Petersen, J. D. *Inorg. Chem.* **1995**, *34*, 821. (b) Pramanik, N. C.; Pramanik, K.; Ghosh, P.; Bhattacharya, S. *Polyhedron* **1998**, *17*, 1525.

Table 3. Electrochemical, IR, and Absorption Data for [**1**](ClO_4), [**2**](ClO_4)$_2$, [**3**](ClO_4), and [**4**](ClO_4)$_3$

	E^o_{298}/V (ΔE_p/mV)[a]				ν/cm^{-1} [b]		
		ligand redn					λ_{max}/nm
compd	Ru^{III}/Ru^{II} couple	NO	dpk	tpy	ClO_4^-	C=O	(ϵ/M^{-1} cm^{-1})[c]
[**1**](ClO_4)	0.88 (70)		−0.95 (100)	−1.41 (120)	1092	1663	588 (5360)
				−1.67 (200)	629		466 sh
							370 sh
							320 (19 500)
							276 (21 900)
							234 (20 400)
[**2**](ClO_4)$_2$	1.37(80)		−0.89 (70)	−1.36 (75)	1092	1666	484 (5970)
				−1.76 (80)	629		408 sh
							328 sh
							306 (27 400)
							276 (28 100)
[**3**](ClO_4)	1.02(120)		−0.99 (100)	−1.60 (70)	1087	1673	508 (6030)
				−1.79 (100)	624		426 (3660)
							332 sh
							312 (27 000)
							274 (27 700)
[**4**](ClO_4)$_3$	n.o.	0.36 (80)	−1.22 (120)	−1.64 (90)	1082	1693	490 sh, br
		−0.35 (130)			634		370 sh
							340 sh
							315 sh
							290 (18 400)
							280 (19 900)
							230 (37 100)
						[**4**]$^{2+}$	520 sh
							487 (1300)
							320 (17 500)
							277 (29 900)
							230 (28 300)
						[**4**]$^{+}$	600 sh
							505 (4600)
							335 sh
							310 (21 400)
							272 (27 900)
							210 (28 100)

[a] From cyclic voltammetry in CH_3CN/Et_4NClO_4, potentials versus SCE, peak potential differences ΔE. [b] In KBr disk. [c] In CH_3CN.

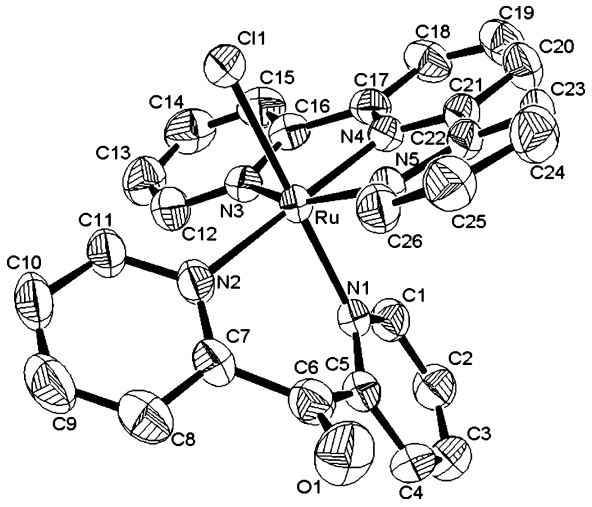

Figure 1. Crystal structure of the cation [Ru(tpy)(dpk)(Cl)]$^+$ of [**1**](ClO_4).

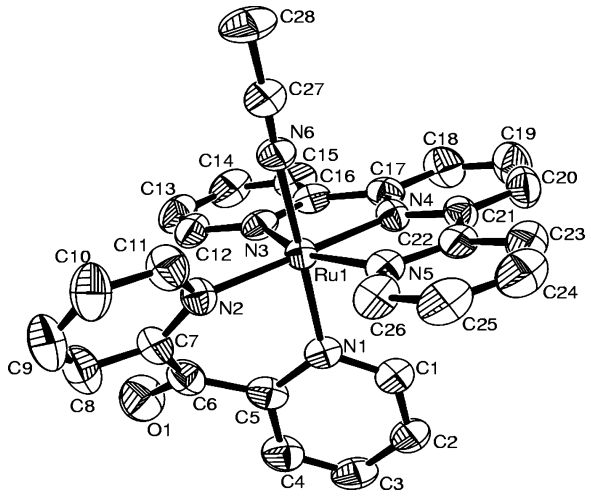

Figure 2. Crystal structure of the dication [Ru(tpy)(dpk)(CH_3CN)]$^{2+}$ of [**2**](ClO_4)$_2$.

chlorate and of the NO_2 ligand with C−H groups of the pyridyl rings of dpk and tpy (Figure S3, Table S3).

The proton NMR spectra of chloro [**1**](ClO_4), acetonitrile [**2**](ClO_4)$_2$, and nitro [**3**](ClO_4) derivatives display the calculated number of 19 partially overlapping signals in the "aromatic region" between 7.0 and 9.8 ppm, 11 resonances for the terpyridine and 8 for the dpk ligand. The data are listed in the Experimental Section, and the spectra are shown in Figure S4. The labile nitrosyl derivative [**4**](ClO_4)$_3$ was found to be partially transformed into the corresponding nitro species during NMR experiment in CD_3CN or $(CD_3)_2SO$, which precluded the recording of an NMR spectrum of the pure nitrosyl complex.

The nitrosyl complex [**4**](ClO_4)$_3$ displays an NO stretching frequency at 1949 cm^{-1} as a strong and sharp band in KBr (Figure S5). This ν_{NO} value of [**4**](ClO_4)$_3$ is higher than values reported for analogous {Ru(tpy)(L)(NO)} complexes

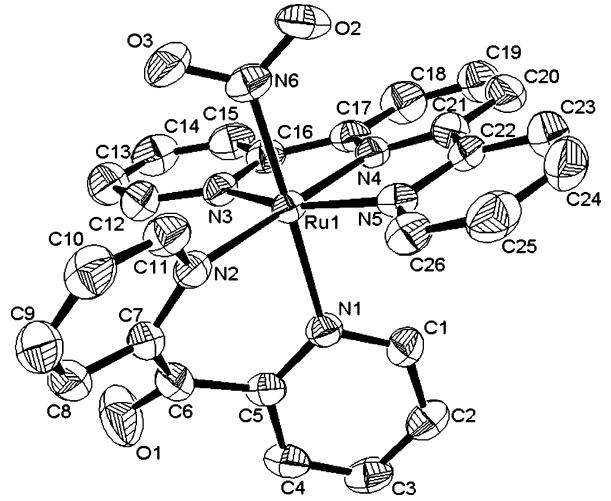

Figure 3. Crystal structure of the cation $[Ru(tpy)(dpk)(NO_2)]^+$ of $[\mathbf{3}](ClO_4)$.

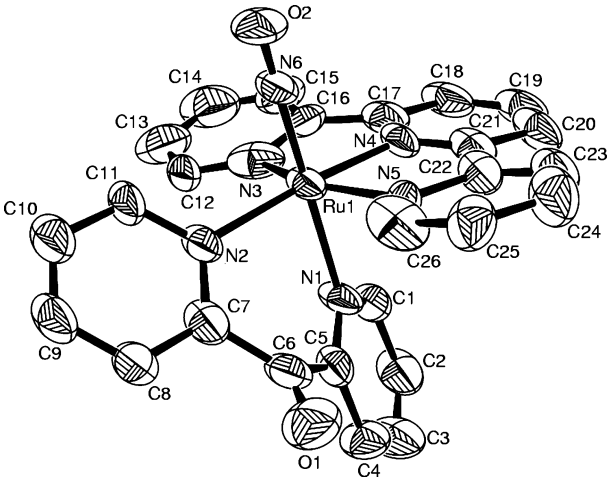

Figure 4. Crystal structure of the trication $[Ru(tpy)(dpk)(NO)]^{3+}$ of $[\mathbf{4}](ClO_4)_3$.

incorporating L = 2-phenylpyridine (1858 cm^{-1}),[15] acetylacetonate (1914 cm^{-1}),[14] and 1-methyl-2-(2-pyridyl)-1*H*-benzimidazole (1932 cm^{-1}).[11] It is closer to values observed for systems with L = 2,2′-bipyridine (1952 cm^{-1}),[12] 2-(2-pyridyl)benzthiazole (1948 cm^{-1}),[11] 2,2′-dipyridylamine (1945 cm^{-1}),[13] or 2-(2-pyridyl)benzimidazole (1944 cm^{-1})[11] and reasonably lower than frequencies observed with L = 2-(2-pyridyl)benzoxazole (1957 cm^{-1})[11] or 2-phenylazopyridine (1960 cm^{-1}).[10] Thus, in the {(tpy)(L)Ru(NO)} framework the ν_{NO} frequency appears to decrease with increasing $d\pi(Ru^{II}) \rightarrow \pi^*(NO^+)$ back-bonding as influenced by the electron-donating ability of the ancillary ligands (L).

The ν(C=O) frequencies of the coordinated dpk ligand (Table 3) show relatively little variation (1668 ± 5 cm^{-1}) except for a noticeable high-energy shift for the higher charged nitrosyl species $[\mathbf{4}]^{3+}$ at 1693 cm^{-1}.

Conversion of $[Ru(tpy)(dpk)(NO)]^{3+}$ to $[Ru(tpy)(dpk)(NO_2)]^+$. Though the nitrosyl complex $[\mathbf{4}](ClO_4)_3$ is reasonably stable in the solid state as well as in dry CH_3CN, it is rapidly transformed into the corresponding nitro derivative when in contact with water. The enhanced electrophilicity of the NO^+ function in $\mathbf{4}^{3+}$ (ν(NO) = 1949 cm^{-1}) via the influence of π-acidic dpk and tpy coligands makes this system susceptible to participate in facile nucleophilic attack. The rate of conversion (eq 1) of the nitroso to the nitro complex was monitored spectrophotometrically in the temperature range 298−318 K in CH_3CN-H_2O (10:1). The well-defined isosbestic points (Figure S6) imply that nitrosyl and nitro species are the main components in the conversion process. The pseudo-first-order rate constant (k), activation parameters ($\Delta H^{\ddagger}/\Delta S^{\ddagger}$), and equilibrium constant (K) are respectively as follows: k/s, 2.46×10^{-4} (298 K), 6.04×10^{-4} (308 K), 1.13×10^{-3} (318 K); 61.98 kJ M^{-1}/−106.5 J K^{-1} M^{-1}; 15.5. The observed large negative $\Delta S^{\ddagger}$ value suggests that the nucleophilec attack of water molecule to the electrophilic nitrosyl center occurs through an associatively activated process.

$$[Ru^{II}(tpy)(dpk)(NO)]^{3+} + H_2O \rightarrow [Ru^{II}(tpy)(dpk)(NO_2)]^+ + 2H^+ \quad (1)$$

Intense ligand-based multiple transitions ($\pi \rightarrow \pi^*$ and n $\rightarrow \pi^*$) are observed in the UV region. Moderately intense metal-to-ligand charge transfer (MLCT) transitions are observed in the visible region for $[\mathbf{1}]^+$, $[\mathbf{2}]^{2+}$, and $[\mathbf{3}]^+$ (Figure S7, Table 3), which are assigned as $d\pi(Ru^{II}) \rightarrow \pi^*$(dpk) and $d\pi(Ru^{II}) \rightarrow \pi^*$(tpy) transitions, respectively.[16c,18] The longer wavelength MLCT transitions of $[\mathbf{1}]^+$ and $[\mathbf{3}]^+$ are due to the negative charge of Cl^- and NO_2^-, which stabilizes occupied metal d orbitals.[22] The higher MLCT band energy for the complex $[\mathbf{4}]^{3+}$ reflects both the positive charge and pronounced π-acceptor characteristics of NO^+. These effects are also illustrated by the metal redox processes (see later). The 7342 cm^{-1} shift in MLCT band energy while moving from X = NO_2^- in $[\mathbf{3}](ClO_4)$ to NO^+ in $[\mathbf{4}](ClO_4)_3$ can be compared to values observed in analogous complexes having L = π-acidic 2,2′-bipyridine (8576 cm^{-1})[12] and strongly π-acidic 2-phenylazopyridine (∼7598 cm^{-1}).[10]

The isolated robust complexes exhibit weakly to moderately strong emission (Figure S8) in EtOH−MeOH (4:1) glass (77 K) on excitation at 500 nm. The emission maxima/quantum yield (ϕ) values are 718 nm/0.015, 626 nm/0.142, and 624 nm/0.034 for $[\mathbf{1}](ClO_4)$, $[\mathbf{2}](ClO_4)_2$, and $[\mathbf{3}](ClO_4)$, respectively. The observed trend for ϕ, X = $CH_3CN > NO_2^- > Cl^-$, shows the effect of the ligand field strength. The emission of ruthenium(II)−polypyridyl complexes is usually attributed to originate from the triplet MLCT state.[19,23,24]

The Ru^{III}/Ru^{II} potentials of $[\mathbf{1}](ClO_4)$, $[\mathbf{2}](ClO_4)_2$, and $[\mathbf{3}](ClO_4)$ vary systematically, depending on the electron donor nature of the monodentate ligand (Figure 5a−c, Table 3). The ligand-based multiple reductions exhibit similar behavior (Table 3), the wave near −1.0 V appearing before the typical

(22) Mondal, B.; Walawalkar, M. G.; Lahiri, G. K. *J. Chem. Soc., Dalton Trans.* **2000**, 4209.
(23) Kar, S.; Chanda, N.; Mobin, S. M.; Datta, A.; Urbanos, F. A.; Puranik, V. G.; Jimenez-Aparicio, R.; Lahiri, G. K. *Inorg. Chem.* **2004**, *43*, 4911.
(24) (a) Sarkar, B.; Laye, R. H.; Mondal, B.; Chakraborty, S.; Paul, R. L.; Jeffery, J. C.; Puranik, V. G.; Ward, M. D.; Lahiri, G. K. *J. Chem. Soc., Dalton Trans.* **2002**, 2097. (b) Juris, A.; Balzani, V.; Barigelletti, F.; Campagna, S.; Belser, P.; Von Zelewsky, A. *Coord. Chem. Rev.* **1988**, *84*, 85.

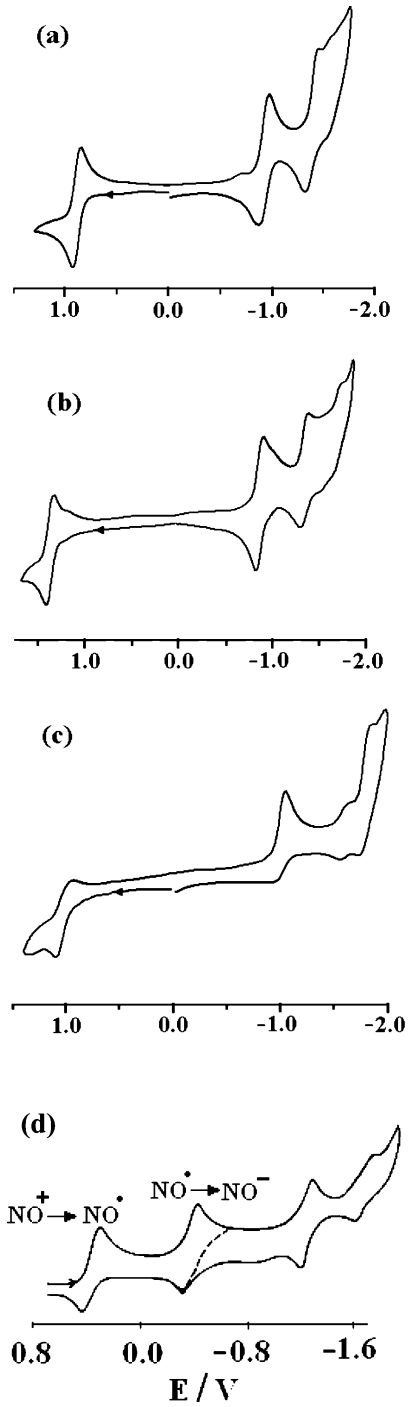

Figure 5. Cyclic voltammograms of (a) [**1**](ClO_4), (b) [**2**](ClO_4)$_2$, (c) [**3**](ClO_4), and (d) [**4**](ClO_4)$_3$ in CH_3CN/0.1 M Et_4NClO_4.

tpy-based reductions between −1.36 and −1.79 V is assigned as the reduction of coordinated dpk.[18,19]

Electrochemistry, EPR, IR, and UV/Vis. Spectroelectrochemistry of the Redox System [4]$^{n+}$. Because of neutrality and the relatively low basicity of the coligands dpk and tpy, the highly charged [**4**]$^{3+}$ ion is reversibly reduced at the rather positive potential of 0.36 V versus SCE in CH_3CN (Figure 5d). Even the second one-electron reduction occurs at the still well accessible potential of −0.35 V. Both potentials are too positive in comparison to those for Ru-coordinated dpk and tpy; the corresponding values for [**4**]$^{(+)\rightarrow(\circ)}$ and [**4**]$^{(\circ)\rightarrow(-)}$ are −1.22 and −1.64 V, respectively. The conclusion that the first two observed waves are due to NO-centered reduction processes is substantiated below. The potential difference of 0.71 V between the successive NO-centered reductions translates to a large comproportionation constant K_c of 10^{12} ($RT \ln K_c = nF(\Delta E)$)[25] for the NO• radical complex intermediate [**4**]$^{2+}$. No oxidation was observed in the accessible potential range.

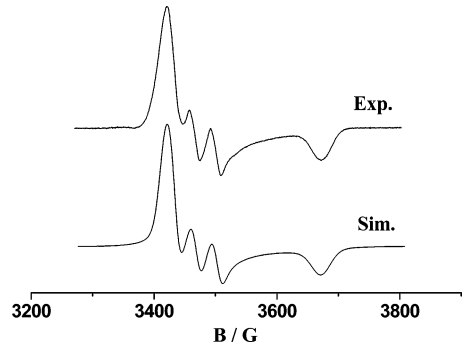

Figure 6. Experimental (top) and computer-simulated (bottom) EPR spectrum of the NO• radical complex **4**$^{2+}$ at 4 K.

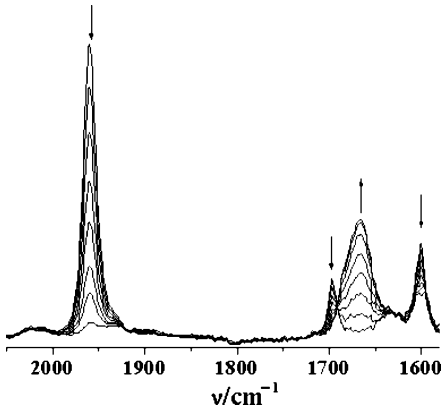

Figure 7. IR spectral changes of processes [**4**]$^{3+}$ → [**4**]$^{2+}$ from OTTLE spectroelectrochemistry in CH_3CN/0.1 M Bu_4NPF_6.

The EPR spectrum of the one-electron-reduced intermediate [**4**]$^{2+}$ in frozen CH_3CN/0.1 M Bu_4NPF_6 yields g components at 2.020 (g_1), 1.993 (g_2), and 1.880 (g_3) with a splitting A_2 of 3.4 mT (Figure 6). These EPR values are well in the range reported recently[26a] for a large number of nitrosylruthenium(II) complexes with widely variable coligands, signifying contributions of about 1/3 from the metal and 2/3 from NO to the singly occupied MO.[26]

Spectroelectrochemistry in the infrared range was also performed in CH_3CN/0.1 M Bu_4NPF_6 solution using an OTTLE cell[27] (see Experimental Section); three pronounced bands in the mid-IR range were studied (Figure 7): (i) The band around 1600 cm^{-1} is ascribed to aryl ring vibrations, and it remains essentially invariant during the reduction process. (ii) The intense band from NO stretching vibration

(25) Creutz, C. *Prog. Inorg. Chem.* **1983**, *30*, 1.
(26) (a) Frantz, S.; Sarkar, B.; Sieger, M.; Kaim, W.; Roncaroli, F.; Olabe, J. A.; Zalis, S. *Eur. J. Inorg. Chem.* **2004**, *14*, 2902. (b) Sieger, M.; Sarkar, B.; Zalis, S.; Fiedler, J.; Escola, N.; Doctorovich, F.; Olabe, J. A.; Kaim, W. *Dalton Trans.* **2004**, 1797. (c) Wanner, M.; Scheiring, T.; Kaim, W.; Slep, L. D.; Baraldo, L. M.; Olabe, J. A.; Zalis, S.; Baerends, E. J. *Inorg. Chem.* **2001**, *40*, 5704.
(27) Krejcik, M.; Danek, M.; Hartl, F. *J. Electroanal. Chem.* **1991**, *317*, 179.

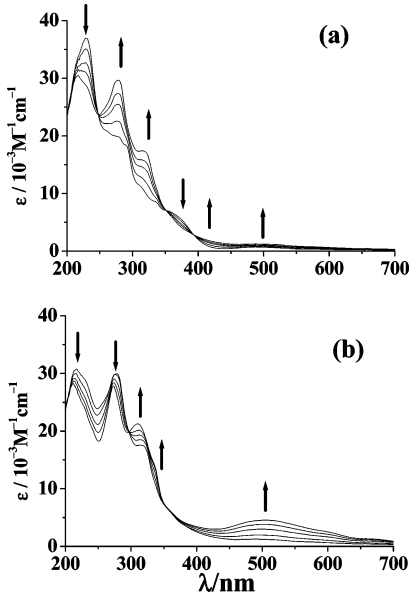

Figure 8. UV−vis spectral changes of (a) $[\mathbf{4}]^{3+} \rightarrow [\mathbf{4}]^{2+}$ and (b) $[\mathbf{4}]^{2+} \rightarrow [\mathbf{4}]^{+}$ from OTTLE spectroelectrochemistry in CH_3CN/0.1 M Bu_4NPF_6.

at 1960 cm^{-1} for $[\mathbf{4}]^{3+}$ shifts to 1666 cm^{-1} during the first reduction to $[\mathbf{4}]^{2+}$. The new band is broad with a high-energy shoulder because of overlap with ν(C═O) from the dpk ligand (cf. below). The very large $\Delta\nu$ of 294 cm^{-1} confirms[26b,c] the NO-centered reduction occurring from an NO^+ ligand state in $[\mathbf{4}]^{3+}$ to an $NO^\bullet$ ligand state in $[\mathbf{4}]^{2+}$. The initial absorption at 1960 cm^{-1} in CH_3CN corresponding to $\nu(NO^+)$ is higher than that observed in KBr (1949 cm^{-1}, Figure S5) due to the presence of only weakly coordinating anions ClO_4^- and PF_6^-. On second reduction, only partially reversible on the time scale of spectroelectrochemistry, the nitrosyl band appears to shift again to lower energies; this spectral region could not be studied because of strong solvent and electrolyte absorption. (iii) The carbonyl stretching band from the dpk at 1697 cm^{-1} shifts to about 1685 cm^{-1} on the first reduction ($[\mathbf{4}]^{3+} \rightarrow [\mathbf{4}]^{2+}$), where it appears as a shoulder to the band of coordinated $NO^\bullet$. On second reduction to $[\mathbf{4}]^+$ it shifts further to 1675 cm^{-1}. These small shifts confirm that dpk does not participate in the reduction process but merely reflects the decreasing overall charge of the complex.

The results from UV/vis spectroelectrochemistry of $[\mathbf{4}]^{3+}$ in CH_3CN/0.1 M Bu_4NPF_6 are shown in Figure 8. In the UV−visible range the spectrum of the precursor $[\mathbf{4}]^{3+}$ exhibits several shoulders (Table 3). The higher energy UV bands are attributed to intraligand (IL) transitions involving the dpk and tpy conjugated π systems. The band (shoulder) at 370 nm is associated with (singlet) MLCT transitions. The origin of the very weak band at about 490 nm is unclear; a triplet MLCT absorption or a typically weak d(M) $\rightarrow \pi^*$-(NO^+) transition[26] can be discussed.

On reduction to the nitrosyl radical complex $[\mathbf{4}]^{2+}$, the absorption intensity in the visible increases slightly and two prominent bands emerge at 320 and 272 nm (Figure 8a, Table 3), possibly associated with transitions involving the above characterized singly occupied MO.

The second reduction to $[\mathbf{4}]^+$ produces a more intense band at 505 nm (Figure 8b, Table 3), which is tentatively assigned to a ligand-to-ligand charge transfer (LLCT) from electron-rich NO^- [28] to π^*(dpk)/(tpy).

Summarizing, we have presented a well-documented series of compounds based on the $[Ru(tpy)(dpk)]^{2+}$ framework which were used to study substitutional and electron-transfer reactivity around the nitrosyl complex $[Ru(tpy)(dpk)(NO)]^{3+}$. The nitrosyl complex and three precursors could be characterized structurally, electrochemically, and by IR and UV−vis spectroscopy (absorption/emission). The conversion from the nitrosyl to the nitro formed could be analyzed kinetically in aqueous medium. In aprotic solution the nitrosyl compound exhibits a two-step reduction via the EPR-active $\{RuNO\}^7$ configuration to the NO^--containing $\{RuNO\}^8$ form with an intense LLCT absorption. Apparently, the $[Ru(tpy)(dpk)]^{2+}$ framework is structurally rigid but electronically sufficiently flexible to allow a convenient monitoring of the conversion of bound nitrosyl.

Experimental Section

Caution! *Special precautions should be taken when handling organic perchlorates.*

The precursor complex $Ru(tpy)Cl_3$ was prepared as reported.[29] 2,2′-Dipyridyl ketone (dpk) and silver perchlorate were purchased from Aldrich, Milwaukee, WI. Other chemicals and solvents were reagent grade and used as received. For spectroscopic and electrochemical studies HPLC grade solvents were used. Solution electrical conductivity was checked using a Systronic conductivity bridge 305. Infrared spectra were taken on a Nicolet spectrophotometer with samples prepared as KBr pellets. ^1H NMR spectra were recorded using a 300 MHz Varian FT spectrometer with $(CD_3)_2SO$ used as solvent for $[\mathbf{1}](ClO_4)$, $[\mathbf{3}](ClO_4)$, and $[\mathbf{4}](ClO_4)_3$ but D_2O for $[\mathbf{2}](ClO_4)_2$. UV−vis spectral studies were performed on a Jasco-570 spectrophotometer. Cyclic voltammetric and coulometric measurements were carried out using a PAR model 273A electrochemistry system. A platinum wire working electrode, a platinum wire auxiliary electrode, and a saturated calomel reference electrode (SCE) were used in a standard three-electrode configuration. Tetraethylammonium perchlorate (TEAP) was used as the supporting electrolyte, and the solution concentration was ca. 10^{-3} M; the scan rate used was 50 mV s^{-1}. A platinum gauze working electrode was used in the coulometric experiments. All electrochemical experiments were carried out under dinitrogen atmosphere. UV−vis and IR spectroelectrochemical studies were performed in CH_3CN/0.1 M Bu_4NPF_6 at 298 K using an optically transparent thin layer electrode (OTTLE) cell[27] mounted in the sample compartment of a Bruins Instruments Omega 10 spectrophotometer and a Perkin-Elmer 1760X FTIR instrument, respectively. The EPR measurements were made in a two-electrode capillary tube[30] with an X-band (9.5 GHz) Bruker system ESP300, equipped with a Bruker ER035M gaussmeter and a HP 5350B microwave counter. The elemental analyses were carried out with a Perkin-Elmer 240C elemental analyzer. Electrospray mass spectra were recorded on a Micromass Q-ToF mass spectrometer. Steady-state emission experiments were done using a Perkin-Elmer LS 55 luminescence spectrometer fitted with a cryostat. For the determination of *k* of

(28) Wanat, A.; Schneppensieper, T.; Stochel, G.; van Eldik, R.; Bill, E.; Wieghardt, K. *Inorg. Chem.* **2002**, *41*, 4.

(29) Indelli, M. T.; Bignozzi, C. A.; Scandola, F.; Collin, J.-P. *Inorg. Chem.* **1998**, *37*, 6084.

(30) Kaim, W.; Ernst, S.; Kasack, V. *J. Am. Chem. Soc.* **1990**, *112*, 173.

the conversion process $[Ru^{II}(tpy)(dpk)(NO)]^{3+} \rightarrow [Ru^{II}(tpy)(dpk)(NO_2)]^{+}$ in acetonitrile−water (10:1) mixture, the increase in absorbance (A_t) at 508 nm corresponding to λ_{max} of the nitro complex was recorded as a function of time (t). A_α was measured when the intensity changes leveled off. Values of pseudo-first-order rate constants, k, were obtained from the slopes of linear least-squares plots of $-\ln(A_\alpha - A_t)$ against t. The activation parameters $\Delta H^{\ddagger}$ and $\Delta S^{\ddagger}$ were determined from the Eyring plot.[31] Quantum yield was calculated with reference to $Ru(bpy)_3^{2+}$ ($\phi = 0.34$).[32]

$[Ru^{II}(tpy)(dpk)(Cl)](ClO_4)$, [1]$(ClO_4)$. A mixture of [Ru(tpy)$Cl_3$] (100 mg, 0.23 mmol), 2,2′-dipyridyl ketone (dpk, 41.8 mg, 0.227 mmol), excess LiCl (54 mg, 1.27 mmol), and NEt_3 (0.4 mL) in 20 mL of ethanol was heated at reflux for 2.5 h under dinitrogen atmosphere. The initial dark brown color gradually changed to deep blue. The solvent was then removed under reduced pressure, and excess saturated aqueous solution of $NaClO_4$ was added to a concentrated acetonitrile solution. The solid precipitate thus obtained was filtered off and washed thoroughly with cold ethanol followed by ice-cold water. The product was dried in vacuo over P_4O_{10}. It was then purified using a silica gel column. The complex [**1**](ClO_4) was eluted by CH_2Cl_2−CH_3CN (8:3) mixture. Evaporation of the solvent under reduced pressure afforded pure [**1**](ClO_4). Yield: 113.5 mg (76%). Anal. Calcd (found): C, 47.79 (47.58); H, 2.93 (2.72); N, 10.72 (10.25). Molar conductivity [Λ_M (Ω^{-1} cm^2 M^{-1})] in acetonitrile: 134. The positive ion electrospray mass spectrum in acetonitrile showed the molecular ion peak centered at m/z = 554.08 corresponding to $\{[\mathbf{1}](ClO_4) - ClO_4\}^+$ (calculated molecular mass: 554.04). ^{1}H NMR (δ/ppm (J/Hz), DMSO-d_6) (Figure S4a): 9.73 (d, 5.1); 8,75 (d, 8.1); 8.69 (d, 7.8); 8.52 (d, 6.9); 8.43 (t, 7.5/7.8); 8.22 (t, 7.8/8.1); 8.08 (multiplet); 7.95 (d, 7.9); 7.82 (t, 7.5/7.6); 7.58 (t, 5.7/6.3); 7.34 (d, 5.4); 7.17 (t, 5.7/6.0).

$[Ru^{II}(tpy)(dpk)(CH_3CN)](ClO_4)_2$, [2]$(ClO_4)_2$. [Ru(tpy)(dpk)(Cl)]$(ClO_4)$, [**1**]$(ClO_4)$ (100 mg, 0.15 mmol), was dissolved in 5 mL of acetonitrile; 25 mL of water was added and the mixture heated to reflux for 5 min. An excess of $AgClO_4$ (320 mg, 1.54 mmol) was then added to the above hot solution, and the heating was continued for 1 h. After cooling, the precipitated AgCl was separated by filtration through a sintered glass crucible (G-4). The volume of the deep-red filtrate was reduced to 10 mL, and a saturated aqueous $NaClO_4$ solution was added in excess. The solid [**2**]$(ClO_4)_2$ thus obtained was filtered off, washed with ice-cold water, and dried in vacuo over P_4O_{10}. Yield: 88.3 mg (76%). Anal. Calcd (found): C, 44.34 (44.23); H, 2.92 (2.83); N, 11.08 (10.56). Molar conductivity [Λ_M (Ω^{-1} cm^2 M^{-1})] in acetonitrile: 239. The positive ion electrospray mass spectrum in acetonitrile showed the molecular ion peak centered at m/z = 657.6 corresponding to $\{[\mathbf{2}](ClO_4)_2 - ClO_4\}^+$ (calculated molecular mass: 658.51). ^{1}H NMR (δ/ppm (J/Hz), D_2O) (Figure S4b): 9.46 (d, 5.1); 8.52 (d, 8.4); 8.41 (multiplet); 8.25 (d, 8.1); 8.19 (d, 5.7); 8.07 (t, 7.8/7.5); 7.98 (d, 6.3); 7.97 (d, 7.8); 7.81 (t, 7.2); 7.51 (t, 6.6/5.4); 7.39 (d, 6.0); 7.08 (t, 6.9/6.6).

$[Ru^{II}(tpy)(dpk)(NO_2)](ClO_4)$, [3]$(ClO_4)$. [Ru(tpy)(dpk)($CH_3CN$)]$(ClO_4)_2$, [**2**]$(ClO_4)_2$ (100 mg, 0.13 mmol), was dissolved in 15 mL of hot water with constant stirring, and an excess of $NaNO_2$ (235 mg, 3.4 mmol) was added. The mixture was then heated to reflux with continuous stirring for 2 h. The deep red solution changed to reddish brown during the course of reaction. The pure crystalline nitro complex precipitated on cooling the solution to room temperature. The solid mass thus obtained was filtered off, washed with ice-cold water, and dried in vacuo over P_4O_{10}. Yield: 65.1 mg (74%). Anal. Calcd (found): C, 47.03 (46.75); H, 2.88 (2.38); N, 12.66 (12.46). Molar conductivity [Λ_M (Ω^{-1} cm^2 M^{-1})] in acetonitrile: 143. The positive ion electrospray mass spectrum in acetonitrile showed the molecular ion peak centered at m/z = 565.1 corresponding to $\{[\mathbf{3}](ClO_4) - ClO_4\}^+$ (calculated molecular mass: 564.5). ^{1}H NMR (δ/ppm (J/Hz), DMSO-d_6) (Figure S4c): 9.05 (d, 5.7); 8.75 (d, 8.1); 8.69 (d, 7.8); 8.45 (multiplet); 8.29 (t, 8.1); 8.14 (multiplet); 8.05 (t, 5.85/6.0); 7.95 (multiplet); 7.64 (t, 6.3/6.9); 7.36 (d, 5.1); 7.29 (t, 7.05/5.4).

$[Ru^{II}(tpy)(dpk)(NO)](ClO_4)_3$, [4]$(ClO_4)_3$. Dropwise addition of concentrated HNO_3 (2 mL) directly to the solid [Ru^{II}(tpy)(dpk)(NO_2)](ClO_4), [**3**](ClO_4) (100 mg, 0.15 mmol), at 273 K under stirring condition resulted in a pasty mass. Ice-cold concentrated $HClO_4$ (6 mL) was then added dropwise under continuous stirring with a glass rod. A yellow solid product was formed on addition of saturated aqueous $NaClO_4$ solution (5 mL). The precipitate was filtered off immediately, washed with ice-cold water (2 mL), and then dried in vacuo over P_4O_{10}. Yield: 107.3 mg (84%). Anal. Calcd (found): C, 36.87 (36.35); H, 2.26 (2.02); N, 9.92 (9.37). Molar conductivity [Λ_M (Ω^{-1} cm^2 M^{-1})] in acetonitrile: 320. The positive ion electrospray mass spectrum in acetonitrile showed the molecular ion peak centered at m/z = 618.04 corresponding to $\{[\mathbf{4}](ClO_4)_3 - NO - 2ClO_4\}^+$ (calculated molecular mass: 618).

Crystal Structure Determination. Single crystals of [**1**](ClO_4) and [**3**](ClO_4) were grown by slow diffusion of an acetonitrile solution of the complex into benzene, followed by slow evaporation. The single crystals of [**2**]$(ClO_4)_2$ or [**4**]$(ClO_4)_3$ were grown via slow evaporation of acetonitrile solutions. X-ray data were collected on a PC-controlled Enraf-Nonius CAD-4 (MACH-3) single-crystal X-ray diffractometer using Mo Kα radiation. Crystal data and data collection parameters are listed in Table 1. The structures were solved and refined by full-matrix least-squares on F^2 using SHELX-97 (SHELXTL).[33] Hydrogen atoms were included in the refinement process as per the riding model. X-ray analysis revealed the presence of one water molecule and two acetonitrile molecules as solvents of crystallization in [**1**](ClO_4) and [**4**]$(ClO_4)_3$, respectively.

Acknowledgment. Financial support received from the Department of Science and Technology, New Delhi, India, the DAAD, the DFG, and the FCI (Germany) is gratefully acknowledged. Special acknowledgment is made to the Sophisticated Analytical Instrument Facility, Indian Institute of Technology, Bombay, India, for providing the NMR facility. X-ray structural studies were carried out at the National Single Crystal Diffractometer Facility, Indian Institute of Technology, Bombay, India.

Supporting Information Available: X-ray crystallographic data for the complexes [**1**](ClO_4), [**2**]$(ClO_4)_2$, [**3**](ClO_4), and [**4**]$(ClO_4)_3$ in CIF format, intermolecular hydrogen bonding of [**1**](ClO_4), [**2**]$(ClO_4)_2$, and [**3**](ClO_4) (Tables S1−S3, Figures S1−S3), ^{1}H NMR spectra of [**1**](ClO_4), [**2**]$(ClO_4)_2$, and [**3**](ClO_4) (Figure S4), the IR spectrum of [**4**]$(ClO_4)_3$ (Figure S5), UV−vis spectra of the conversion $[\mathbf{4}]^{3+} \rightarrow [\mathbf{3}]^{+}$ (Figure S6), electronic spectra of [**1**](ClO_4), [**2**]$(ClO_4)_2$, [**3**](ClO_4), and [**4**]$(ClO_4)_3$ (Figure S7), and emission spectra of [**1**](ClO_4), [**2**]$(ClO_4)_2$, and [**3**](ClO_4) (Figure S8). This material is available free of charge via the Internet at http://pubs.acs.org.

IC050533E

(31) Wilkins, R. G. *The study of kinetics and mechanism of reaction of Transition MetalComplexes*; Allyn and Bacon: Boston, MA, 1974.
(32) (a) Alsfasser, R.; van Eldik, R. *Inorg. Chem.* **1996**, *35*, 628. (*b*) Chen, P.; Duesing, R.; Graff, D. K.; Meyer, T. J. *J. Phys. Chem.* **1991**, *95*, 5850.
(33) Sheldrick, G. M. *Program for Crystal Structure Solution and Refinement*; Universität Göttingen: Göttingen, Germany, 1997.